J Mater Sci: Mater Electron (2013) 24:1274–1281
DOI 10.1007/s10854-012-0918-z

The role of Lu doping on microstructural and superconducting properties of $Bi_2Sr_2CaLu_xCu_2O_y$ superconducting system

O. Ozturk · E. Asikuzun · G. Yildirim

Received: 25 July 2012 / Accepted: 20 September 2012 / Published online: 4 October 2012

Abstract Lutetium (Lu) added $Bi_2Sr_2CaLu_xCu_2O_y$ superconducting samples with x = 0, 0.1, 0.3, 0.5, 0.7 and 1.0 are prepared by solid-state reaction method and annealed at 840 °C for 50 h. The heating and cooling rates of the furnace are adjusted to be 10 and 3 °C/min, respectively. For the comparison, undoped sample is subjected to the same annealing conditions. The prepared samples are characterized using X-ray powder diffraction (XRD), scanning electron microscope (SEM), energy dispersive spectroscopy (EDS), and dc resistivity ($\rho-T$) measurements. The volume fraction, grain size, texturing and lattice parameters are determined from the XRD measurements. The microstructure, surface morphology and element composition analysis of the samples produced are investigated by SEM and EDS measurements, respectively. Moreover, the resistivity (at room temperature), critical transition (onset and offset) temperature, variation of transition temperature and hole carrier concentration values of the samples studied are estimated from the dc resistivity measurements. According to the results obtained, the samples prepared exhibit the polycrystalline superconducting phase with less intensity of diffraction lines with the enhancement in the Lu addition due to the effect of the minor phase (Bi-2201). The lattice parameter *c* and volume fraction of Bi-2212 phase reduce systematically whereas the cell parameter *a* and minor phase fraction enhance with ascending the Lu content in the system, leading to the decrement in the superconducting properties. Scanning electron microscope measurements show that not only do the surface morphology and grain connectivity degrade but the grain sizes of the samples decrease with the increase of the Lu addition, as well. Energy dispersive spectroscopy results reveal that the Lu^{3+} ions might enter into the crystal structure by replacing Sr^{2+} ions, confirming why the superconducting properties of the pure sample are more superior to the samples doped. At the same time, dc resistivity results obtained show that the room temperature resistivity systematically increases with the enhancement of the Lu content as a result of the hole filling when the onset (T_c^{onset}) and offset (T_c^{offset}) temperatures determined from the resistivity curves decrease from 99.5 to 93.0 K and 85.0 to 60.0 K, respectively, illustrating not only the increment in the relative percentage of Bi-2201 phase formation and the reduction of the mobile carrier concentration but also the presence of impurities and weak links between the superconducting grains.

O. Ozturk (✉) · E. Asikuzun
Department of Physics, Kastamonu University,
37100 Kastamonu, Turkey
e-mail: oozturk@kastamonu.edu.tr

G. Yildirim
Department of Physics, Abant Izzet Baysal University,
14280 Bolu, Turkey

1 Introduction

As well known the first superconductor containing the bismuth element with the critical temperature (T_c) of 20 K was discovered by Mitchell et al. [1] in 1987. In this year, calcium oxide was introduced in this system by Maeda et al. [2]. Surprisingly, the critical temperature of this new compound was found to be around 110 K. The general formula of this system is $Bi_2Sr_2Ca_{n-1}Cu_nO_{2n+4}$ obtaining three different phases with respect to its chemical compositions, the Bi-2201 phase ($n = 1$, $T_c \approx 20$ K), the Bi-2212 phase ($n = 2$, $T_c \approx 85$ K) and the Bi-2223 phase ($n = 3$, $T_c \approx 110$ K) [3]. Here,

n values denote the number of the CuO planes due to the layered structure of the system. As understood, the critical transition temperature enhances with the increment of the CuO planes. All the phases are the same as structurally expect for the number of CuO and Ca planes. However, the preparation of the single phase is a very difficult task as a consequence of the high complexity of the reaction and the appearance of numerous phases during the phase formation [4, 5]. Additionally, several preparation conditions such as the annealing ambient (time, temperature atmosphere and pressure), composition, type and quantity of the chemicals, heat-treatment and operational procedures affect the phase formation. A small change in the conditions can lead to damage the structure. Thus, the superconducting properties (critical temperature, critical current density etc.) change positively or vise versa.

Sometimes, the rare earth addition in the high temperature superconductors such as YBCO, BSCCO leads to important changes in microstructural, electrical and mechanical properties. The rare earth can exhibit ferromagnetic, antiferromagnetic and paramagnetic properties at different temperature as a result of the participation of electron in the 4f orbital. To illustrate, holmium (Ho) shows ferromagnetic below the 20 K, antiferromagnetic between the 20 and 133 K and paramagnetic properties over the 133 K. Hence, the rare earth elements are the most promising materials for potential technological and industrial applications. Moreover, Lutetium (Lu) metal discovered by Georges Urbain and Baron Carol Auer von Welsbach in 1907 is another interesting rare earth element with its atomic number of 71 and atomic weight of 174.967. Within the Lanthanide series, this element obtains the smallest atomic radius (175 pm) and the highest melting temperature (1652 °C). In the last decades, the researches on Lutetium and its oxidized compounds have increased owing to these characteristics [6–8].

In this study, the microstructural, electrical and superconducting properties of the Lutetium doped Bi-2212 superconducting materials prepared by the solid-state reaction method were investigated by X-ray diffraction (XRD), scanning electron microscopy (SEM), energy dispersive spectrometer (EDS) and electrical resistivity ($\rho-T$) measurements. X-ray diffraction measurements for the phase composition, texturing and lattice parameters; SEM and EDS pictures for microstructure examination and element composition; electrical resistivity measurements for electrical and superconducting properties of the Lu added Bi-2212 superconducting samples were performed, respectively. It is found that the electrical, microstructural and superconducting properties are dependent sensitively upon the Lu doping in the Bi-2212 system.

2 Experimental details

In previous work [9], we analyzed the mechanical properties of the Lu doped Bi-2212 superconducting ceramics of nominal composition of $Bi_2Sr_2CaLu_xCu_2O_y$, with x = 0.0, 0.1, 0.3, 0.5, 0.7 and 1.0. The sample preparation procedure and the Vickers micro hardness, elastic modulus, load independent hardness, yield strength, fracture toughness and brittleness index values were discussed in detail elsewhere [9]. Hereafter, we will use the abbreviation Lu0.0, Lu0.1, Lu0.3, Lu0.5, Lu0.7 and Lu1.0.

In the present study, the significant changes of the microstructural and superconducting properties of the same samples were investigated with the help of the X-ray powder diffraction (XRD), scanning electron microscope (SEM), energy dispersive spectroscopy (EDS) and resistivity ($\rho-T$) measurements.

X-ray diffraction measurements were carried out using a Bruker D8 Advance model XRD diffractometer with CuKα target giving a monochromatic beam with wavelength 1.54 Å in the range $2\theta = 8°–60°$ at a scan speed of 3°/min and step increment of 0.02° at room temperature. The lattice parameter, texturing and volume fraction values were extracted from the XRD patterns. The accuracy in determining the lattice parameters (*a* and *c*) was found to be ± 0.0001 Å. Additionally, the average grain sizes of the samples studied were calculated by the Scherrer–Warren approach using XRD peaks [10–12].

The grain size, grain connectivity and surface morphology of the samples were determined using a Jeol scanning electron microscope (SEM) JEOL 6390-LV, operated at 20 kV, with a resolution power of 3 nm. Moreover, EDS (Energy dispersive spectrometer) was used to investigate the elemental compositions (in the percent).

The electrical properties of the samples were examined by dc resistivity versus temperature measurements using 5 mA dc current through the samples in a closed-cycle cryostat in the temperature range from 40 to 120 K. Both voltage and current contacts were made with silver paint contact to reduce contact resistance. A Keithley 220 programmable current source and a Keithley 2182A nanovoltmeter system were used for the conventional four-probe measurements.

3 Result and discussion

3.1 XRD analysis

Figure 1 shows the room temperature powder X-ray diffraction (XRD) peaks between 8° and 60° for the $Bi_2Sr_2CaLu_xCu_2O_y$ ceramics with x = 0.0, 0.1, 0.3, 0.5, 0.7 and 1.0. With the help of the diffraction patterns the texture,

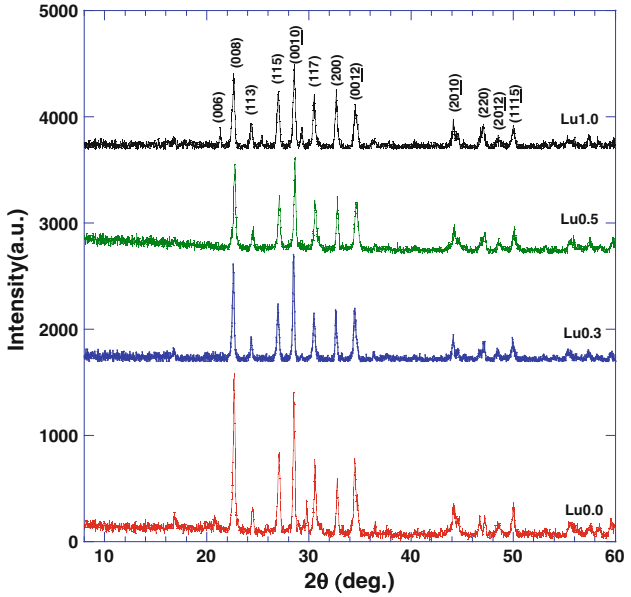

Fig. 1 XRD patterns of the Lu0.0, Lu0.1, Lu0.3, Lu0.5, Lu0.7 and Lu1.0 samples

phase fraction, grain size and lattice constant parameters of the Bi-2212 superconductors with and without Lu content are determined and compared with each other. The corresponding (*h k l*) Miller indices belonging to Bi-2212 main lines are shown in the diagrams of Fig. 1. It is visible from the figure that both pure and Lu-added samples are mainly composed of perovskite based Bi-2212 phase and so the peaks depicted in the figure are indexed on the basis of the Bi-2212 (major phase) structure. Besides, all the samples studied exhibit the polycrystalline superconducting phase with less intensity of diffraction lines with the enhancement in the Lu addition as a consequence of the appearance of the minor phases. In other words, the peak intensities belonging to the Bi-2212 phase reduce while that of the minor phase enhances systematically with ascending the Lu addition in the system, presenting that why the superconducting properties degrade with the doping. The relative percentages of Bi-2212 and Bi-2201 phases are calculated by means of the relations (1) and (2) and are tabulated in Table 1.

$$f_{(2212)} = \frac{\sum I_{2212(hkl)}}{\sum I_{2212(hkl)} + \sum I_{2201(hkl)}} \quad (1)$$

and

$$f_{(2201)} = \frac{\sum I_{2201(hkl)}}{\sum I_{2212(hkl)} + \sum I_{2201(hkl)}} \quad (2)$$

where *I* gives the peak intensity of the present phase. As seen from the table that the relative percentage of the Bi-2212 phase decreases from 85 to 59 % whereas that of the Bi-2201 phase increases from 15 to 41 %, respectively. It is another important point obtained from the figure that no secondary phase containing oxide composition, Lu, Lu_2O_3 or any other cation is observed for all the samples, indicating that the Lu^{+3} ions are incorporated into the crystal structure of Bi-2212 superconductor [13–15]. As for the cell structure of the samples prepared, the cell parameters *a* and *c* are computed using the least square method through *d* values and (*h k l*) planes for tetragonal unit cell structure. The variation of the lattice parameters *a* and *c* inferred from the XRD graphs of the samples studied is displayed in Table 1. One can see from the table that a systematic elongation in the *a*-axis length is obtained while a regular contraction in the *c*-axis length is observed with the addition, confirming that the Lu^{3+} ions might enter into the crystal structure by replacing Sr^{2+} ions. In the literature, the similar results have been observed with the presence of the rare earth in the system [16–21]. According to the results obtained, it is clear that although the Bi-2212 phase decreases while the Bi-2201 phase starts to increase with the Lu addition in the system, Fig. 1 confirms that the Bi-2212 phase is dominant for the samples prepared, being ascertained by both the resistivity and SEM measurements.

3.2 Grain size calculation

The determination of particle size is very important to examine the effect of doping on the crystallite size of

Table 1 Lattice parameter *a* and *c*, volume fraction, grain size and hole concentration of all the samples

Samples	*a* (Å)	*c* (Å)	Volume fraction (%)		Grain Size (nm)	Hole Concentration (*p*)
			2212	2201		
Lu0.0	5.382	30.67	85	15	50.32	0.143
Lu0.1	5.389	30.64	68	32	46.11	0.121
Lu0.3	5.394	30.45	65	35	37.65	0.119
Lu0.5	5.397	30.21	64	36	37.17	0.118
Lu0.7	5.405	30.01	62	38	32.36	0.116
Lu1.0	5.412	29.59	59	41	31.64	0.100

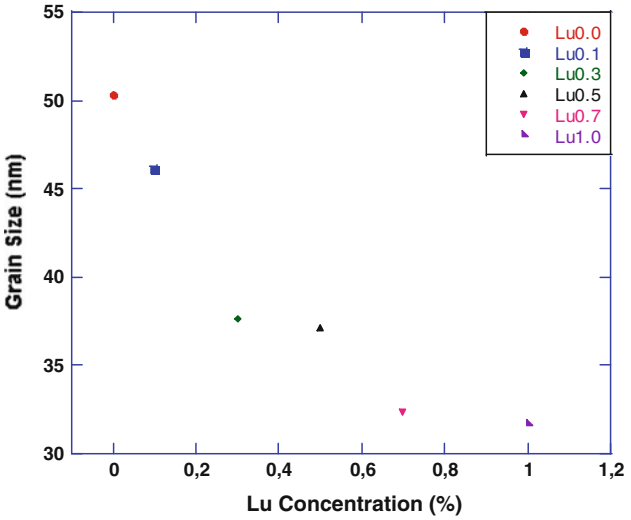

Fig. 2 Variation of grain size versus Lu-Content for all samples

materials. Grain size of samples can be calculated with the aid of the X-ray diffraction patterns using Scherrer–Warren equation [22–24].

$$D = {}^{0.941\lambda}/_{\beta \cos \theta_\beta} \quad (3)$$

where D denotes grain size (nm), λ is the wave length of X-ray (0.154 nm), β presents the FWHM of the highest intensity peak and θ is the corresponding angle of the peak. The grain sizes calculated are summarized in Table 1. As seen from the table and Fig. 2, the average grain size of samples decreases with the increment of the Lu doping, being favored by the SEM investigations.

3.3 SEM analysis

Surface structure analysis of the samples prepared was performed by scanning electron microscopy (SEM). It is realized that there is a systematic change in the micrographs (taken in the secondary electron image mode at 5000-X magnification) of the fractured surfaces and thus we give only the micrographs of the Lu0.0 (the best surface) and Lu1.0 (the worst surface) sample in Fig. 3a, b to indicate the main differences between them. According to the figure, the microstructures of the samples studied are surprisingly different from each other. The surface of the former sample is observed to be much smoother and denser with larger grain size compared to that of the latter sample. Moreover, the sample obtains more uniform surface appearance, lower porosity, better crystallinity and connectivity between grains than to the latter one, presenting that why the superconducting properties degrade with the increase of the Lu addition. Based on these results obtained, it is obvious that the microstructure of the Bi-2212 phase strongly depends on the Lu addition and in fact the grain connectivity and grain size deteriorate as a result of the presence of the Lu^{3+} ions in the Bi-2212 system.

3.4 EDS analysis

The elemental composition analyses of the samples prepared in this work are analytically investigated by the energy dispersive spectrometer (EDS) investigations. Similar to the SEM results, we give only the element concentration of Lu0.0 and Lu1.0 samples in Fig. 4. It is observable from the figure that no difference appears between the two samples studied except for the Lu peak, confirming that the Lu^{3+} ions are successfully introduced to the microstructure of the Bi-2212 phase [25]. Furthermore, the element concentration dependence on the Lu content is displayed in Fig. 5. One can see from the figure that Bi, Ca and O compositions in all the samples are variable while the level of Cu increases with the enhancement of the Lu content. On the other hand, the Sr compositions compared to other element compositions decrease rapidly with the increase in the Lu doping in the system (Table 2). Based on the results of EDS, the Lu^{3+} ions

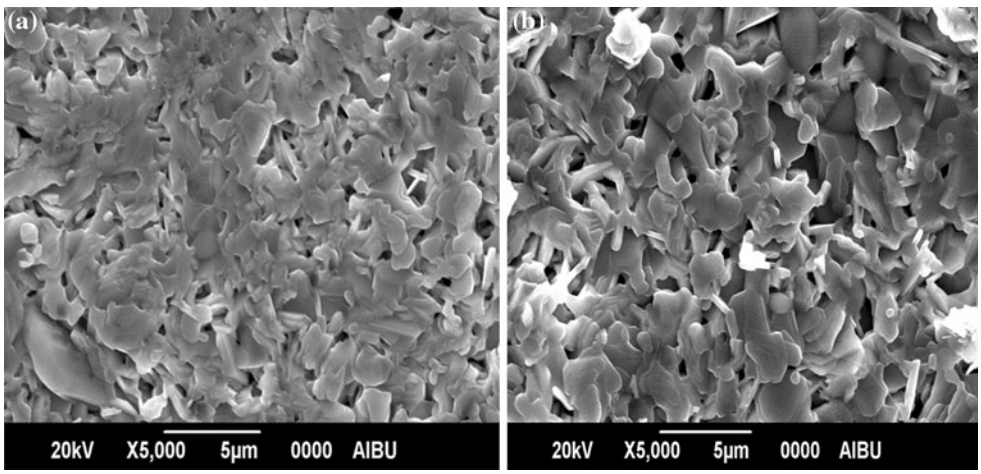

Fig. 3 SEM micrographs of **a** Lu0.0 and **b** Lu1.0 samples

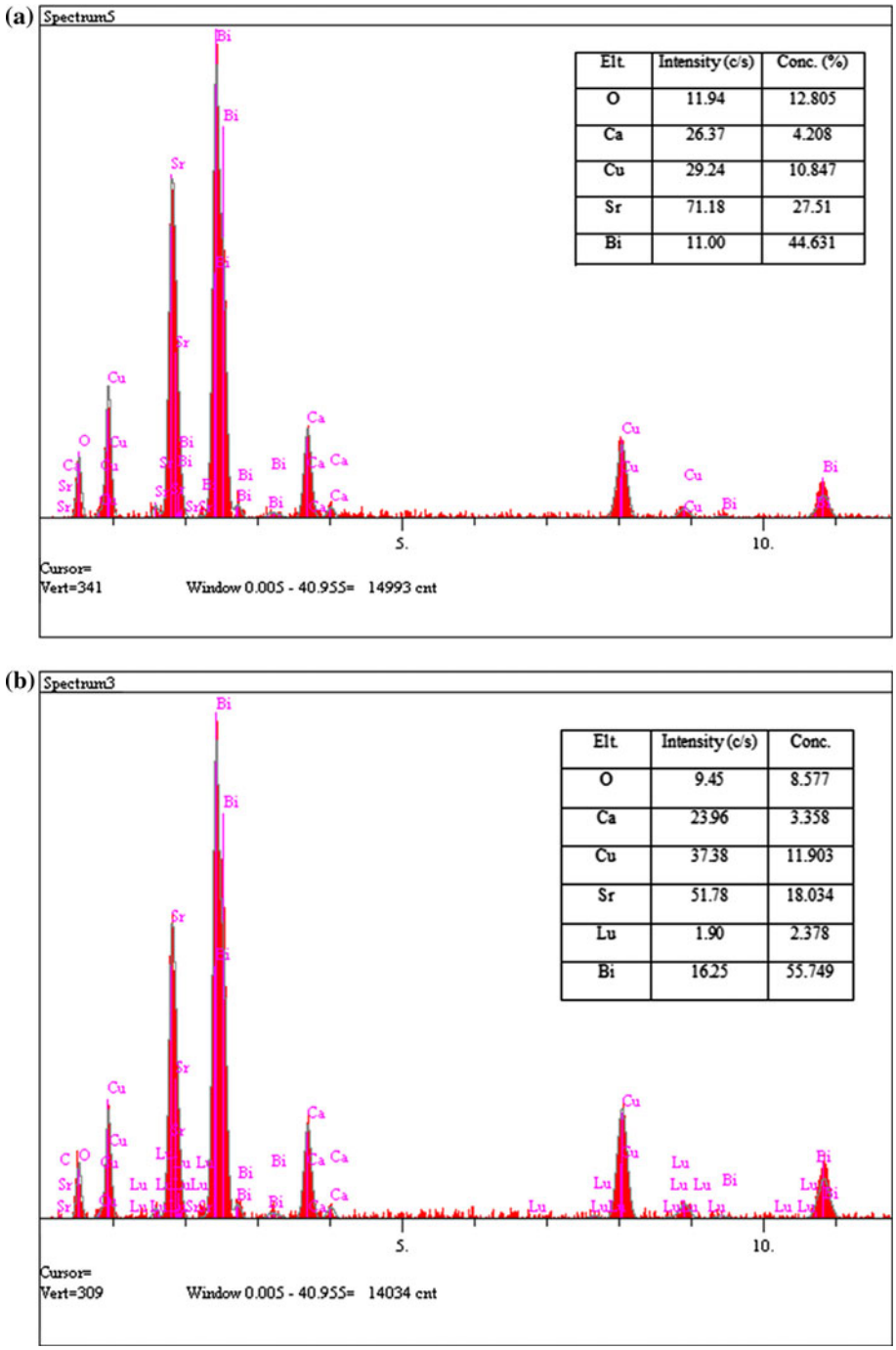

Fig. 4 Results of EDS measurements of **a** Lu0.0 and **b** Lu1.0 samples

were determined to enter into the crystal structure by replacing Sr^{2+} ions [26], confirming that why the superconducting properties of the pure sample are more superior to the other samples.

3.5 Resistivity measurements

The role of the Lu doping on superconductivity properties of Bi-2212 superconducting materials studied in this work, dc electrical resistivity is measured as a function of temperature in the range of 50–120 K and the results observed are given in Fig. 6. It is observed that the resistivity curves obtained exhibit a transition to the superconducting state below the superconducting onset temperature (T_c^{onset}) above which all the samples show metallic behavior. The normal state resistivity is observed to regularly increase with the enhancement of the Lu addition to a maximum resistivity of 42 Ω μm for x = 1.0 as against 5 Ω μm for the pure sample (Table 3). When the Lu^{3+} ions are doped the Bi-2212 system, each doping of Lu^{3+} starts

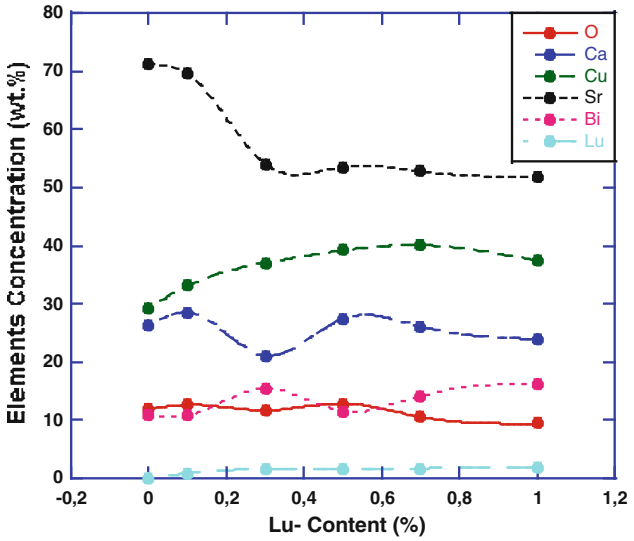

Fig. 5 Variation of the element concentration as a function of Lu addition level

Table 2 Concentrations of the elements of the samples studied

Component	Concentration (wt%)					
	Lu0.0	Lu0.1	Lu0.3	Lu0.5	Lu0.7	Lu1.0
O	11.94	12.68	11.71	12.88	10.58	9.450
Ca	26.37	28.56	21.13	27.45	26.12	23.96
Lu	–	0.910	1.620	1.690	1.730	1.900
Cu	29.24	33.23	37.03	39.22	40.09	37.38
Sr	71.18	69.53	53.99	53.56	52.78	51.78
Bi	11.00	10.85	15.47	11.54	14.19	16.25

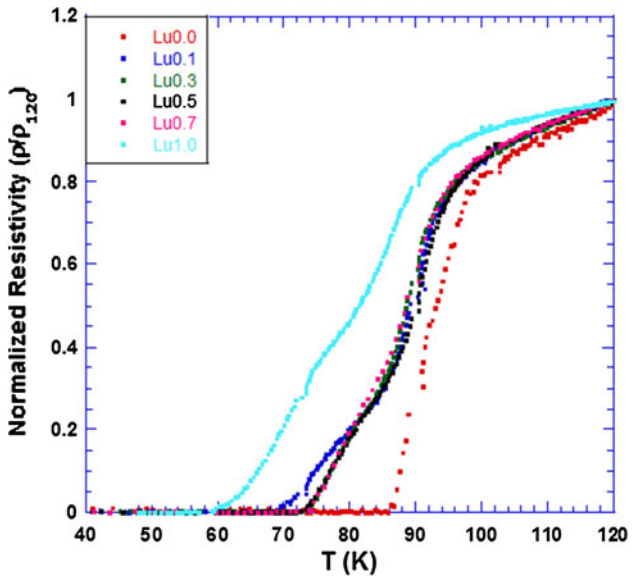

Fig. 6 Normalized resistivity as a function of temperature curves for the samples

to fill the hole in the crystal. Thus, the hole filling takes place and normal-state resistivity of the system increases monotonously [27, 28]. An increase in the resistivity is attributed to the reduction of the charge carrier concentration in the Cu–O_2 plane with the Lu addition in the system as a consequence of a general nature for all the rare earth elements [29–32]. At the same time, the onset critical (T_c^{onset}) and offset critical (T_c^{offset}) temperatures evaluated from Fig. 6 are listed in Table 3. According to the literature, the former is associated with the transition of isolated grains to the superconducting state; on the other hand, the latter is attributed to the volume fraction of Bi-2212 phase and/or features of intergranular component [33–35]. Table 3 gives that both the T_c^{onset} and T_c^{offset} values decrease from 99.5 to 93.0 K and 85.0 to 60.0 K, respectively as the Lu addition enhance in the system due to both the increment in the relative percentage of Bi-2201 phase formation and the reduction of the mobile carrier concentration. To analyze in detail the superconducting properties and weak links between the grains, the variation of the critical transition temperature (T_c^{offset}) versus Lu-Content is pictured in Fig. 7. It is apparent from the figure that the T_c^{offset} value decreases dramatically for the Lu0.1 sample; however, the slight decrement of the T_c^{offset} values is observed for the Lu0.3, Lu0.5 and Lu0.7 samples. As for the Lu1.0 sample, a sharp decrease in the T_c^{offset} is obtained. This phenomenon might stem from the basis of the change in hole-concentration (carrier doping state) due to the Lu addition at Sr-site of the Bi-2212 superconducting samples prepared [36, 37]. Additionally, this study reports the variation (ΔT_c) between the critical transition temperatures for all the samples studied and the ΔT_c values determined are given in Table 3. It is evident from the table that the variation enhances significantly from 14.5 to 33.0 K with ascending the Lu content in the Bi-2212 system because of both the presence of impurities, porosities and weak links between the superconducting grains [38, 39], being favored by the SEM images.

3.6 Carrier concentration calculation

The hole-carrier concentrations per Cu ion, p, are calculated by use of the following relation [40–42]:

$$P = 0.16 - \left[\left(1 - \frac{T_c}{T_c^{\mathrm{Max}}}\right)/82.6\right]^{1/2} \quad (4)$$

where T_c^{max} is received as 85 K [9] for Bi-2212 system, p denotes hole concentration when T_c is taken from Table 3. In this work, the p values calculated are tabulated in the same table. It is visible that the hole carrier concentration decreases from 0.143 to 0.100 with the increment of the Lu addition in the system. Figure 8 also shows

Table 3 Some physical characteristics of the samples prepared

Samples	T_c^{onset} (K)	T_c^{offse} (K)	ΔT_c (K)	Room temperature resistivity ρ (Ω μm)
Lu0.0	99.5	85.0	14.5	5
Lu0.1	97.0	74.0	23.0	15
Lu0.3	96.0	73.5	22.5	16
Lu0.5	94.0	73.0	21.0	18
Lu0.7	94.0	72.0	22.0	33
Lu1.0	93.0	60.0	33.0	42

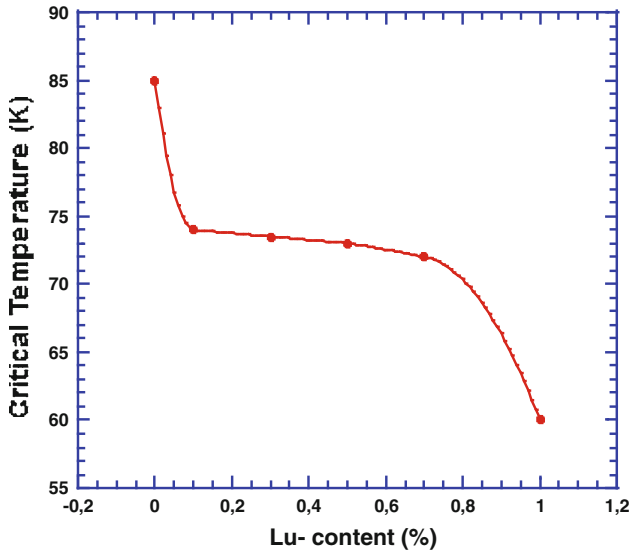

Fig. 7 Variation of critical temperature versus Lu-Content for all samples

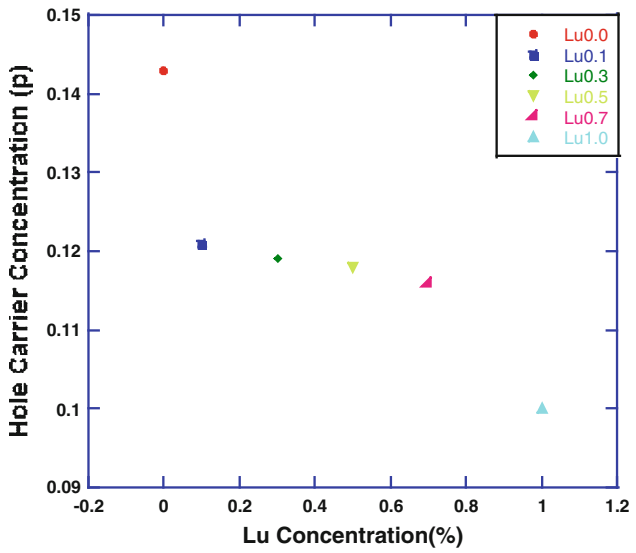

Fig. 8 Variation of hole-carrier concentrations versus Lu-Content for all samples

the relationship between the Lu content and the p values. According to the figure, there is a sharp decrease up to the addition ratio of 0.1 % beyond which the slight reduction is observed to 0.7 % addition ratio. However, the dramatic decrement is repeated for the Lu1.0 sample. This may be related to the fact that the considerable decrease in the grain size results from both the presence of the excess (Lu^{+3}) ion effect and the appearance of the minor phases in the Bi-2212 system.

4 Conclusion

In our study, the role of Lu doping on the microstructural, electrical and superconducting properties of Bi-2212 superconductors prepared by solid-state reaction method is investigated by the XRD, SEM, EDS and $\rho-T$ measurements. The resistivity curves allow us to analyze the room temperature resistivity, onset and offset critical temperature, variation of transition temperature and hole-carrier concentration values of the samples; similarly, we determine the volume fraction, grain size, texturing and lattice parameters from the XRD measurements. Moreover, surface morphology, crystallinity and element distribution of the samples produced are examined by means of the SEM and EDS measurements. The results of dc resistivity measurements indicate that with the enhancement of the Lu content in the Bi-2212 system the room temperature resistivity regularly increases due to the hole filling. The T_c^{onset} and T_c^{offset} values decrease from 99.5 to 93.0 K and 85.0 to 60.0 K, respectively as a result of the increment in the relative percentage of Bi-2201 phase formation and the reduction of the mobile carrier concentration. A considerable increase in the ΔT_cvalues with the Lu addition points out the presence of impurities and weak links between the superconducting grains. X-ray powder diffraction results also demonstrate that the Bi2212 ceramics prepared in this work exhibit the polycrystalline superconducting phase with less intensity of diffraction lines with increasing the Lu addition due to the enhancement in the phase fraction of Bi-2201. The reduction of the lattice parameter c also confirms the increase of the minor phase fraction in the system. Additionally, SEM images present that the surface morphology and grain connectivity degrade monotonously as the Lu addition increase. Energy dispersive spectroscopy measurements also picture that the Lu^{3+} ions might enter into the crystal structure by replacing Sr^{2+} ions, confirming that why the superconducting properties decrease with the Lu doping in the Bi-2212 system. To sum up, the electrical, microstructural and superconducting properties of the Bi-2212 bulk superconductor samples are dependent strongly upon the Lu content.

Acknowledgments The author thanks to Prof. Dr. A. Varilci and Prof. Dr. C. Terzioglu for their advices and enlightening comments on this work. And also this study is dedicated to his newborn son of Gurcan Yildirim.

References

1. G.W. Mitchell, M. Herviev, M.M. Borel, A. Grandin, F. Deslandes, J. Provost, B. Raveav, Z Phys B **68**, 421 (1987)
2. H. Maeda, Y. Taraka, Jpn. Appl. Phys. **27**, L209 (1987)
3. J.M. Tarascon, Y. Lepage, L.H. Greene, B.G. Bagley, P. Barboux, D.M. Hwang, G.W. Hull, W.R. Makinnon, M. Girond, Phys. Rev. B **38**, 2504 (1988)
4. E. Giannini, E. Bellingeri, R. Passerini, R. Flukiger, Physica C **315**, 185 (1999)
5. G. Yildirim, S. Bal, E. Yucel, M. Dogruer, M. Akdogan, A. Varilci, C. Terzioglu, J. Supercond. Nov. Magn. **25**, 381 (2012)
6. C.F. Liu, F. Ye, L.M. Liu, Y. Zhou, J. Alloy. Compd. **475**, 735 (2009)
7. P. Berastegui, S.G. Eriksson, L.G. Johanson, J. Alloy. Compd. **252**, 76 (1997)
8. P.M. Sarun, S. Vinu, R. Shabna, J.B. Anooja, P.M. Aswathy, U. Syamaprasad, IEEE T. Appl. Supercond. **20**, 61 (2010)
9. O. Ozturk, M. Erdem, E. Asikuzun, O. Yildiz, G. Yildirim, A. Varilci, C. Terzioglu, Mater. Sci Mater. Electron. (2012). doi:10.1007/s10854-012-0722-9
10. B.D. Cullity, *Elemt of X-ray Diffraction*, 3rd edn. (Addition-Wesley, Reading MA, 2001)
11. E. Asikuzun, O. Ozturk, H.A. Cetinkara, G. Yildirim, A. Varilci, M. Yilmazlar, C. Terzioglu, J. Mater. Sci.: Mater. Electron. **23**, 1001 (2012)
12. P.M. Sarun, S. Vinu, R. Shabna, A. Biju, U. Syamaprasad, Mater. Res. Bull. **44**, 1017 (2009)
13. S. Vinu, P.M. Sarun, A. Biju, R. Shabna, P. Guruswamy, U. Syamaprasad, Supercond. Sci. Technol. **21**, 045001 (2008)
14. S. Vinu, P.M. Sarun, R. Shabna, A. Biju, U. Syamaprasad, Mater. Lett. **62**, 4421 (2008)
15. R. Shabna, P.M. Sarun, S. Vinu, A. Biju, U. Syamaprasad, Supercond. Sci. Technol. **22**, 045016 (2009)
16. G. Yildirim, E. Yucel, S. Bal, M. Dogruer, A. Varilci, M. Akdogan, C. Terzioglu, Y. Zalaoglu, J. Supercond. Nov. Magn. **25**, 231 (2012)
17. H. Wang, A. Serquis, B. Maiorov, L. Civale, Q.X. Jia, P.N. Arendt, S.R. Foltyn, J.L. Macmanus-Driscoll, X. Zhang, J. Appl. Phys. **100**, 053904 (2006)
18. S. Vinu, P.M. Sarun, R. Shabna, A. Biju, U. Syamaprasad, Mater. Chem. Phys. **119**, 135 (2010)
19. A. Biju, U. Syamaprasad, A. Rao, J.G. Xu, K.M. Sivakumar, Y.K. Kuo, Physica C **466**, 69 (2007)
20. O. Ozturk, E. Asikuzun, S. Kaya, M. Coskunyurek, G. Yildirim, M. Yilmazlar, C. Terzioglu, J. Supercond. Nov. Magn. (2012). doi:10.1007/s10948-012-1673-3
21. O. Ozturk, J. Mater. Sci.: Mater. Electron. **23**, 1235 (2012)
22. L. Shi, Y. Gu, L. Chen, Z. Yang, J. Ma, Y. Qitan, Mater. Lett. **58**, 3301 (2004)
23. J. Jiang, Mater. Lett. **61**, 3239 (2007)
24. O. Ozturk, E. Asikuzun, M. Erdem, G. Yildirim, O. Yildiz, C. Terzioglu, J. Mater. Sci.: Mater. Electron. **23**, 511 (2012)
25. S. Bal, M. Dogruer, G. Yildirim, A. Varilci, C. Terzioglu, Y. Zalaoglu, J. Supercond. Nov. Magn. **25**, 847 (2012)
26. A. Biju, P.M. Sarun, R.P. Aloysius, U. Syamaprasad, J. Alloy. Compd. **454**, 46 (2008)
27. M.A. Ansari, R. Nigam, V.P.S. Awana, A. Gupta, R.B. Saxena, H. Kishan, N.P. Lalla, V. Ganesan, A.V. Narlikar, C.A. Cardoso, J. Appl. Phys. **97**, 10B104 (2005)
28. Y. Zalaoglu, G. Yildirim, C. Terzioglu, J. Mater. Sci.: Mater. Electron. (2012). doi:10.1007/s10854-012-0723-8
29. R.P. Aloysius, P. Guruswamy, U. Syamaprasad, Supercond. Sci. Technol. **18**, L23 (2005)
30. A. Biju, R.P. Aloysius, U. Syamaprasad, Supercond. Sci. Technol. **18**, 1454 (2005)
31. V.G. Prabitha, A. Biju, R.G. Abhilashkumar, P.M. Sarun, R.P. Aloysius, U. Syamaprasad, Physica C **433**, 28 (2005)
32. A. Biju, R.P. Aloysius, U. Syamaprasad, Physica C **440**, 52 (2006)
33. D. Yazici, M. Erdem, B. Ozcelik, J. Supercond. Nov. Magn. **25**, 725 (2012)
34. O. Ozturk, T. Kucukomeroglu, C. Terzioglu, J. Phys.: Condens. Matter **19**, 346205 (2007)
35. R. Lortz, T. Tomita, Y. Wang, A. Junod, J.S. Schilling, T. Masui, S. Tajima, Physica C **434**, 194 (2006)
36. P.M. Sarun, S. Vinu, R. Shabna, A. Biju, U. Syamaprasad, Mater. Lett. **62**, 2725 (2008)
37. T. Motohashi, Y. Nakayama, T. Fujita, K. Kitazawa, J. Shimoyama, K. Kishio, Phys. Rev. B **59**, 14080 (1998)
38. O. Ozturk, H.A. Cetinkara, E. Asikuzun, M. Akdogan, M. Yilmazlar, C. Terzioglu, J. Mater. Sci.: Mater. Electron. **22**, 1501 (2011)
39. A. Ianculescu, M. Gartner, B. Despax, V. Bley, Th Lebey, R. Gavrila, M. Modreanu, Appl. Surf. Sci. **253**, 344 (2006)
40. M.F. Azzouz, A. Mchirgui, B. Yangui, C. Boulesteix, B.M. Salem, Physica C **356**, 83 (2001)
41. K. Kocabas, S. Sakiroglu, M. Ciftcioglu, I. Ercan, H. Epik, O. Bilgili, J. Supercond. Nov. Magn. **22**, 749 (2009)
42. M.R. Persland, J.L. Tallon, R.G. Buckley, R.S. Liu, N.E. Floer, Physica C **176**, 95 (1991)